Bioactive Materials 35 (2024) 291–305

Contents lists available at ScienceDirect

Bioactive Materials

journal homepage: www.keaipublishing.com/en/journals/bioactive-materials

Effect of chitin-architected spatiotemporal three-dimensional culture microenvironments on human umbilical cord-derived mesenchymal stem cells

Shuoji Zhu [a], Junfeng Xuan [b], Yunchao Shentu [b], Katsuhiko Kida [c], Masaki Kobayashi [c], Wei Wang [d], Minoru Ono [a,**], Dehua Chang [b,*]

[a] Department of Cardiac Surgery, University of Tokyo, Tokyo, 113-8655, Japan
[b] Department of Cell Therapy in Regenerative Medicine, University of Tokyo Hospital, Tokyo, 113-8655, Japan
[c] Nissan Chemical Corporation, Tokyo, 103-0027, Japan
[d] Winhealth Pharma, 999077, Hong Kong

ARTICLE INFO

Keywords:
Cellhesion® chitin nanoscaffolds
Mesenchymal stem cells
Stemness
3D culture

ABSTRACT

Mesenchymal stem cell (MSC) transplantation has been explored for the clinical treatment of various diseases. However, the current two-dimensional (2D) culture method lacks a natural spatial microenvironment *in vitro*. This limitation restricts the stable establishment and adaptive maintenance of MSC stemness. Using natural polymers with biocompatibility for constructing stereoscopic MSC microenvironments may have significant application potential. This study used chitin-based nanoscaffolds to establish a novel MSC three-dimensional (3D) culture. We compared 2D and 3D cultured human umbilical cord-derived MSCs (UCMSCs), including differentiation assays, cell markers, proliferation, and angiogenesis. When UCMSCs are in 3D culture, they can differentiate into bone, cartilage, and fat. In 3D culture condition, cell proliferation is enhanced, accompanied by an elevation in the secretion of paracrine factors, including vascular endothelial growth factor (VEGF), hepatocyte growth factor (HGF), Interleukin-6 (IL-6), and Interleukin-8 (IL-8) by UCMSCs. Additionally, a 3D culture environment promotes angiogenesis and duct formation with HUVECs (Human Umbilical Vein Endothelial Cells), showing greater luminal area, total length, and branching points of tubule formation than a 2D culture. MSCs cultured in a 3D environment exhibit enhanced undifferentiated, as well as higher cell activity, making them a promising candidate for regenerative medicine and therapeutic applications.

1. Introduction

Mesenchymal stem cells (MSC) are derived from mammalian mesenchymal tissue and can self-renew in an undifferentiated state and differentiate into various types of somatic cells, including adipocytes, osteocytes and chondrocytes [1]. MSCs also have the property of secreting immune regulatory factors [2], which provides research inspiration and ideal prospects for stem cells and regenerative medicine [3]. However, the effects of MSC therapy are still heterogeneous and lack explanation mechanisms, which may be attributed to the inconsistency of cell sources, functional characteristics, and culture methods [4]. It is particularly noteworthy that keeping MSCs in an undifferentiated state in long-term culture, especially the rapid establishment and stable maintenance of MSC stemness, remains challenging [5]. Detachment from the native three-dimensional microenvironmental structure and signals may be an important reason for the heterogeneity of MSCs *in vitro* [6,7]. Therefore, replicating the interaction between cells and the natural microenvironment *in vitro* is expected to provide feasible cytological solutions [8,9].

The native umbilical cord MSC (UCMSC) is easily attainable and expanded *in vitro*, and it has been shown stronger proliferative capacity and lower immunogenicity than MSCs derived from other tissues, such as bone marrow, peripheral blood, and fat [10]. Due to the convenience of extraction, a large number of source cells, and significant immunomodulatory properties, UCMSC has been regarded as one of the active

Peer review under responsibility of KeAi Communications Co., Ltd.
* Corresponding author.
** Corresponding author.
E-mail addresses: ONO-THO@h.u-tokyo.ac.jp (M. Ono), jou.sur@mail.u-tokyo.ac.jp (D. Chang).

https://doi.org/10.1016/j.bioactmat.2024.01.014
Received 16 November 2023; Received in revised form 11 January 2024; Accepted 15 January 2024

Abbreviations

UCMSC	Umbilical cord mesenchymal stem cell
MSC	Mesenchymal stem cell
HUVEC	Human Umbilical Vein Endothelial Cells
VEGF	Vascular endothelial growth factor
HGF	Hepatocyte growth factor
IL-6	Interleukin-6
IL-8	Interleukin-8
ELISA	Enzyme-linked immunosorbent assay
CFU	Colony forming unit
RNA	Ribonucleic acid
DNA	Deoxyribonucleic acid
MCM	Minichromosome maintenance
ATP	Adenosine triphosphate
GO	Gene ontology
EV	sExtracellular vesicle

"seeds" with sound therapeutic potential [11]. Moreover, UCMSCs can be frozen and stored long-term; it is also possible to establish a cell bank according to uniform sample selection and a standard operating procedure to support cell therapy. Preserving the physical functions of multifunctional cells like UCMSCs with high fidelity *in vitro* provides fundamental support for molecular mechanism research and translational application of regenerative medicine [12]. The use of advanced three-dimensional (3D) rather than two-dimensional (2D) culture methods has been shown to provide enlightening auxiliary strategies [13]. In-depth bioanalysis of the characteristics of biomaterial-based 3D culture systems will not only elucidate the *in vitro* adaptability of UCMSCs but also essentially elucidate the communication network between stem cells and the surrounding environment that triggers effective tissue homeostasis and damage repair [14,15]. Therefore, appropriate tissue engineering 3D culture and cell property assessment can help improve the quality control of standardized therapeutic UCMSC.

In local tissues, interactions between stem cells and the microenvironment, whether caused by cellular activity [16] or niche dynamics [17,18], may be a critical upstream factor in tissue repair. Recent studies have shown that biomaterials can improve the biological properties of UCMSCs, including self-renewal [19], differentiation [20], and paracrine delivery [21]. This is a desirable direction for the development of UCMSC therapeutics. However, the precise cell biology involved remains vague [22], given the specific gene expression and heterogeneity of cell subpopulations in MSCs [23]. In addition, because umbilical cord mesenchymal tissue, the native habitat of UCMSCs, has complex structural components such as blood vessels, mucus, and connective tissue [24], the 3D biomimetic conditions and functions of biomaterials must be further explored. To direct a functional biome assessment of UCMSC 3D culture systems, and especially to identify the responding genetic patterns, will therefore be instructive.

To maintain high cell viability, morphology, stemness, and paracrine stability of UCMSCs *in vitro*, we previously developed a 3D culture system based on bioactive chitin materials called Cellhesion® [25]. Cellhesion® has tissue engineering properties, including biocompatibility, biodegradability, and high mechanical strength, providing an emerging biomaterial platform for regeneration [26]. By constructing an artificial UCMSC–Cellhesion® biome system, we have developed new *in vitro* methodologies to evaluate the quality of UCMSCs. This study found that the UCMSC–Cellhesion® system provided a unique microenvironment through spherical tissue formation and cell stability establishment as the chitin scaffold degraded. Through analysis of stem cell marker proteins and genomic RNA expression, the early systematic activity of Cellhesion®-cultured UCMSC was revealed. Cellhesion®'s cell-niche dynamic interaction resulted in higher UCMSC stability and stemness maintenance, compared to a 2D culture. This study provides valuable scientific insights into the basic extension and translation feasibility of UCMSC-based therapy.

2. Materials and methods

2.1. Human UCMSC culture

For the 2D culture, primary UCMSCs (PromoCell, cat. No. C-12971) were cultured in petri dishes at 37 °C, 5 % CO_2, and 95 % humidity. The cells were kept in an MSC growth medium (Promo Cell, Heidelberg, Germany) with 10 % (v/v) FBS (Life, NY, USA) and a 1 % (v/v) antibiotic-antimycotic solution. The medium was changed every three days. Cells were passaged with Hepes BSS (Promo Cell, Heidelberg, Germany), 0.04 % (w/v) trypsin-EDTA (Promo Cell, Heidelberg, Germany), 0.05 % Trypsin inhibitor 0.1 % BSA (Promo Cell, Heidelberg, Germany) when they reached 80–90 % confluency. For the 3D culture of UCMSCs (second passage), the culture material was prepared by adding 0.05 % (v/v) Cellhesion® (Nissan Chemical Co., Ltd., Tokyo, Japan) to the above medium, in accordance with the manufacturer's instructions. The material was then seeded in 100 ml non-adherent flasks (Corning, NY, USA) at a density of 1×10^6 UCMSCs/flask. This 3D cell system was cultured at 5 % CO_2 and 37 °C, and the medium was changed every three days by centrifugation (cells along with materials, 100 g/min for 5 min) and resuspension.

2.2. Cell viability and proliferation assays (with Cellhesion®)

To analyze the survival and proliferation of cells cultured *in vitro*, we used placental blue fluorescence staining to measure the cell number of UCMSCs at the fourth passage, comparing cells in the 3D Cellhesion® environment to those in the 2D environment. Following the manufacturer's instructions, the Embryonic Blue stain (Invitrogen, USA) and Embryonic Blue cell counter (Invitrogen, USA) were employed for standardized quantification of cell numbers in the cultures. Cell expansion was analyzed using a serial assay of cell counting. The 2D group utilized 24-well adhesion culture plates, with each well containing 2×10^5 cells/ml cells and 2 ml of cell culture medium (Promp Cell, Germany). The 3D group used 24-well non-adhesion culture plates, with each well containing 2×10^5 cells, 1.9 ml of culture medium, and 100 μl of Cellhesion material. Cultured up to 5 days, data were obtained daily and analyzed with Prism software using SEM for comparison between 3D and 2D groups.

2.3. UCMSCs exported from the 3D environment

After seven days of culture in Cellhesion® 3D, the UCMSCs were transferred to the to Petri dishes with adhesive properties to establish the effect of the 3D culture on cell proliferation. Typically, the culture medium was centrifuged at 500 g/min for 5 min, then resuspended and dropped into a 100 mm adhesive petri dish. The isolates were cultured statically for 24 h, allowing UCMSCs to detach from the 3D material and adhere to the dish. Next, 10 ml of UCMSCs culture medium was added to the dish, and then the Cellhesion® material was gradually washed away through multiple medium changes.

2.4. Cell viability and proliferation assays (after removing UMSCs from Cellhesion®)

UCMSCs crawled out from the Cellhesion® 3D environment and were transferred to a six-well adherent culture dish at a concentration of 1×10^5 cells/ml and cultured continuously for five days. During this period, UCMSC counting was performed every day, using the Embryonic Blue stain and Embryonic Blue cell counter. Statistics of daily cell numbers ($N = 3$) were used to generate proliferation curves. Cultured for up to 5 days, data were obtained daily and analyzed with Prism software

using SEM for comparison between 3D and 2D groups.

2.5. Scanning electron microscopy (SEM) evaluation

Scanning electron microscopy (SEM) was used to study the physical interaction between UCMSCs and 3D materials. Precisely, a 0.1 M phosphate buffer (pH 7.4) containing 2 % formaldehyde and 2.5 % glutaraldehyde was used to preliminarily fix the 2D or 3D culture cells, with 1 % osmium tetroxide and 0.5 % potassium ferrocyanide added for secondary fixation. Ethanol, tert-butanol, and freeze-drying were used for fractionated dehydration, and osmium tetroxide was used to coat the dry samples. The morphological characteristics were observed using an S-4800 field emission SEM (Hitachi High-Technologies, Japan).

2.6. MSC adipogenic differentiation

To test whether the Cellhesion® material affects the adipocyte differentiation potential of UCMSCs, the 3D cultured fourth passage UCMSCs were seeded into a six-well culture dish at a concentration of 1 $\times$ 10^5 cells/ml. When the cells reached 90 % confluence, the original medium was replaced with MSC^{tm}_{go} adipogenic medium (Sartorius), and culture was continued at 37 °C and 5 % CO_2. The medium was changed every three days. On day 21 the cells were fixed with formaldehyde and stained with an oil-red solution (BMK Bio Future Workshop Corporation, Tokyo, Japan) for 30 min. The stained population was observed using a 10 $\times$ microscope.

2.7. MSC osteogenic differentiation

In the fourth passage, UCMSCs cultured in 2D and 3D environments were prepared with cell suspension at a concentration of 1 $\times$ 10^5 cells/ml and seeded in six-well adherent culture dishes, respectively. When the cells reached 80 % confluence, the culture medium was replaced with an osteogenic medium (Osteogenic Differentiation Culture Solution, Sartorius), and the culture was continued at 37 °C with 5 % CO_2. The medium was changed every three days. On day 14 the osteogenic medium was removed and the cells were fixed with fixative for 30 min, in accordance with the osteogenic staining kit instructions (BMK Bio Future Workshop Corporation). Alizarin Red S dye from the kit was then used to stain the cells for 30 min. After washing four times with PBS, the staining of differentiated osteoblasts was observed under a 10 $\times$ microscope.

2.8. MSC chondrogenic differentiation

The fourth passage UCMSCs cultured in 2D and 3D environments were prepared with cell suspension at a concentration of 1 $\times$ 10^6 cells/ml and seeded in six-well adherent culture dishes, respectively. A 2 ml cartilage culture solution (Cartilage Differentiation Culture Solution, Sartorius) was applied to each well. The lines were then incubated in a cell culture chamber at 37 °C with 5 % CO_2, and the culture medium was refreshed every three days. On day 14, the cells were stained using Alcian blue (BMK Bio Future Workshop Corporation) for 15 min. After washing four times with PBS to remove residual dye, a 10 $\times$ microscope was used to observe cell differentiation.

2.9. Immunophenotype analysis

We evaluated the stemness of UCMSCs cultured with Cellhesion® according to the MSC phenotype criteria established by the International Society for Cell Therapy [16]. Cells were incubated with CD73, CD90, CD105, CD11b, CD19, CD34, CD45, and DLA-DR antibodies following the antibody reagent manufacturer's instructions (BD Biosciences, USA). UCMSCs were centrifuged at 300 g/min for 5 min and washed twice with SM buffer (2 % FBS in PBS). Eight tubes of cell suspension were prepared, with a concentration of 5–10 $\times$ 10^6 cells/ml. Cells were centrifuged at a 300 g/min speed for 5 min. SM buffer solution (50 μL) was then used for resuspension. Cells and antibodies were incubated at room temperature for 30 min in the dark. We added 1 ml SM buffer, centrifuged at 300 g/min for 3 min at 4 °C four times, and added propidium iodide. Antibody-labeled cells were sent to FACS Aria II (BD Biosciences) and flow cytometry data were analyzed using FlowJo software (Tree Star, San Carlos, CA, USA).

2.10. Enzyme-linked immunosorbent assay (ELISA) of cell culture supernatants

The protein levels of hepatocyte growth factor (HGF; cat. No. KAC2211, Thermo Fisher Scientific), vascular endothelial growth factor (VEGF; cat. No. P35235, Funakoshi, Japan), Interleukin-6 (IL-6; cat. No. 350580, Funakoshi, Japan), and Interleukin-8 (IL-8; cat. No. P352238, Funakoshi, Japan) in 2D and 3D culture media were measured using the ELISA Kit (Funakoshi). Supernatants from fourth-passage UCMSCs, 2D and 3D culture media (Promocell, Germany) were collected every day for seven days. In a 96-well culture dish, we added 150 μL of incubation buffer, 50 μL of Standard Diluent Buffer, and 50 μL of either the experimental or control sample. We beat it gently to mix the complex and left it untouched for 3 h. We removed the supernatant, washed it four times with PBS, added 100 μL/well of biotin anti-Hu HGF (VEGF), and left it untouched for 1 h. After discarding the supernatant, we added 100 μL Streptavidin-HRP (100-fold dilution) to each well and left the dish untouched at room temperature for 30 min. We then added 100 μL stop solution and mixed until the solution turned yellow, measured by 450 nm fluorescence. All reagents were tested within 2 h.

For IL-6 and IL-8, we added 100 μL Assay Diluent RD1W to each well of an adhesive 96-well culture dish, followed by a 100 μL supernatant sample, leaving the dish untouched at room temperature for 2 h. We then washed the well four times with 400 μL PBS and added IL-6 Conjugate. The dish was kept in the dark and left untouched at room temperature for 2 h. The well was then washed four times with 400 μL PBS, 200 μL substrate solution was added, and it was kept in the dark for 20 min. Finally, 50 μL stop solution was added to turn the solution green, followed by analysis by a spectrophotometer with fluorescence absorbances of 450 nm, 540 nm, and 570 nm. The detection process of all targets was completed within 30 min.

The results were analyzed and statistical analyses were conducted using Prism software, with standard deviation (SD) employed to compare the 3D results with the 2D group.

2.11. Tube formation assay

We used Matrigel, which was thawed and mixed with HUVEC culture medium EBM-2 (Clonetics, USA, without additives) at a ratio of 2:1. Subsequently, 95 μL of the mixture was added to each well, followed by the addition of 20,000 HUVEC cells (the fourth passage) and either 200 μL 3D or 2D Day-5 conditioned medium. Two control groups were set as 200 μL MSC culture medium (Mesenchymal Stem Cell Growth Medium 2, PromoCell, Germany) and 200 μL HUVEC culture medium (including culture medium additive EBM-2, Clonetics, USA). Apart from comparing the advantages of Cellhesion®'s 3D cell culture, this experimental design also allowed for eliminating potential interference and confounding factors from the culture medium. After 12 h, the formation of lumens was observed, recorded, and analyzed. The vascular area and length were quantified and annotated using Image-J software, followed by statistical analysis using Prism software. Standard Deviation (SD) was used for analyzing the statistical significance compared to the 2D group.

2.12. Colony formation assay

At the fourth passage, UCMSCs were seeded at a concentration of 20,000 cells/ml into a 10 cm ultra-low adhesion culture dish containing 0.05 % (w/v) Cellhesion® MS using Mesenchymal Stem Cell Growth

Medium 2 nourish. The culture supernatant was changed every three days. The plates were incubated without agitation for one week. The UCMSCs were then adhered and separated from Cellhesion® using a conventional 10 cm diameter petri dish. The isolated UCMSCs were inoculated into the middle 60 wells of a conventional 96-well plate, with one cell placed in each well. FBS (−) was added peripherally to maintain the environmental stability and humidity of the culture dish. The proliferating clones were observed by culturing them in a cell incubator for seven days. Meanwhile, colony forming unit (CFU) experiments were performed simultaneously on a 2D control, without the addition of Cellhesion® but according to the above culture criteria.

2.13. Cell cycle analysis

The fourth passage UCMSCs cultured in the 2D and 3D culture media were prepared as previously described. Then, 2×10^6 UCMSCs cultured in 2D and 3D were delivered to and stored at BGI Japan (Tokyo). Total mRNA was isolated using the BGI Japan kit, and RNA-Seq was conducted using the DNBSEQ platform. Two replicated RNA-seq libraries were prepared from UCMSCs cultured in 2D and 3D. The sequencing data was filtered with SOAP nuke (v1.5.6) by removing adopter reads, low-quality reads, and reads whose unknown base ('N' base) ratio exceeded 5 %. Clean reads were obtained and stored in FASTQ format and were mapped to the reference genome using HISAT2 (v2.1.0). Bowtie2 (v2.3.4.3) was applied to align the clean reads to the gene set. RSEM (v1.3.1) calculated the expression level of the gene. A heatmap was generated by pheatmap (v1.0.8). A differential expression analysis was performed using DESeq2 (v1.4.5) with $|\log2FC| \geq 2.5$, FDR ≤ 0.001, and visualized by an enhanced volcano (v3.16). GO (http://www.geneontology.org/) and KEGG (https://www.kegg.jp/)

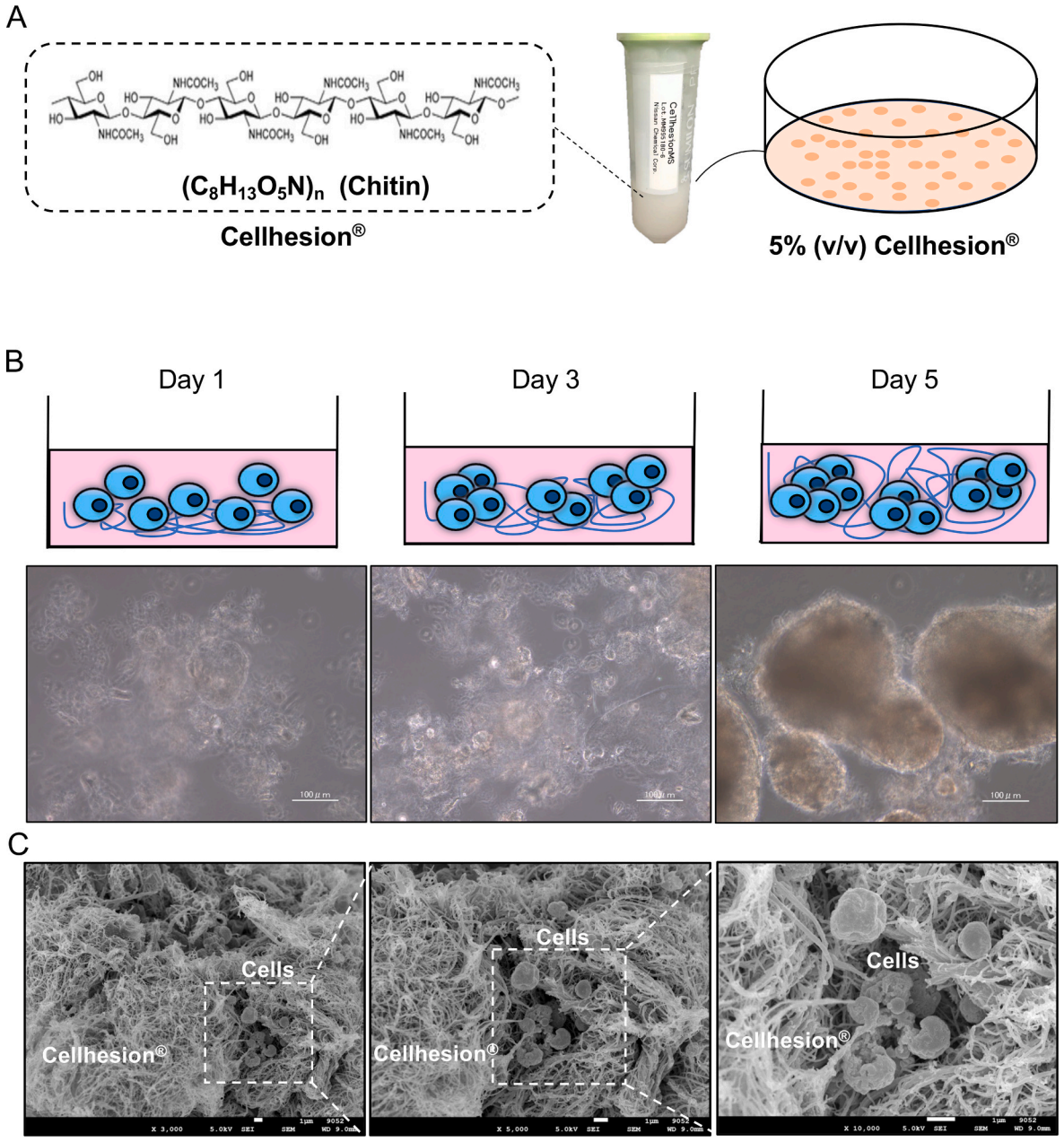

Fig. 1. The culture of UCMSCs with Cellhesion®. (A) Cellhesion® is a white flocculent-like liquid consisting mainly of chitin. It is added to the culture medium to form a 3D environment with a concentration of 5 %. (B) Over time, Cellhesion® forms a 3D matrix in which materials and cells are gradually included into larger clusters, as shown in the figures for Day 1, Day 3, and Day 5. (C) The spatial relationship between the MSCs and Cellhesion®. The magnifications from left to right are 3000×, 5000×, and 10000×. Within the white dashed line is the UCMSC, which can be seen clustering and enveloped by the Cellhesion® material.

enrichment analyses of annotated different expression genes were performed by Phyper, based on the hypergeometric test. The significant levels of terms and pathways were corrected by Q value with a rigorous threshold (Q value ≤ 0.05).

2.14. Statistical analyses

Cell proliferation was presented as mean ± SEM, Elisa data and CFU data as mean ± SD of at least three independent determinations. Prism software was used for statistical analysis and image visualization of cell staining and chemiluminescence readings. Statistical analysis between groups was performed using unpaired two-tailed Student's t-test (or ANOVA). Differences were considered significant when $p < 0.05$.

3. Results

3.1. Characteristics of Cellhesion® compound cell culture

In accordance with Cellhesion®'s product instructions, the cells were added to the cell culture medium at a concentration of 0.05 % and well homogenized to establish a 3D culture environment for the cells (Fig. 1A). While in the 3D culture setting, UCMSCs coexisted within the Cellhesion® culture matrix and progressively formed spherical aggregates, with discernible growth in aggregate size over time (Fig. 1B), as demonstrated in Cellhesion® VP enhancing the immunomodulatory potential of human mesenchymal stem cell-derived extracellular vesicles. In contrast to conventional 2D culture, the 3D petri dishes exhibited a slightly turbid appearance due to the inclusion of biomaterials (Fig. 2A). By the fifth day, these aggregates had become readily visible. Through electron microscopy, we observed that UCMSCs exist in a spherical state within the three-dimensional Cellhesion® material and have adapted to exist in such a 3D environment (Fig. 1C).

3.2. Proliferation of 2D and 3D cultured cells

To compare the growth of UCMSCs under 2D and 3D culture conditions, they were seeded on adherent tissue culture plates and in non-adherent tissue culture flasks and analyzed using the placental blue staining assay. Cell counts were taken daily for five days. On the fourth day, the average count for the 2D culture was 747,000 cells and 569,333 cells for the 3D culture. The proliferation of UCMSCs in the presence of Cellhesion® material was less than in the 2D culture conditions. This disparity persisted during the culture period, even though the cells exhibited exponential growth. By the fifth day, the average cell counts were 1,238,333 for 2D culture and 621,333 for 3D culture. On that day, the cells peaked (Fig. 2B). Notably, by the fifth day, the cells and the 3D material remained integrated, with the 3D material forming larger clusters. The placental blue assay revealed that, although both cultures peaked on the fifth day, the proliferation of UCMSCs within the 3D material was less than that under conventional 2D culture conditions. The results of this experiment agree with the summary of a Polish review, which reported that because of the structure of cell spheroids, the reasons for differences in nutrients could lead to limitations in the spheroid culture of hepatocytes [27].

3.3. Cellhesion® post-culture and cell proliferation

To account for the impact of Cellhesion® material aggregation on cell proliferation rates and to validate the effect of Cellhesion® material on cell performance. Consequently, 3D culture UCMSCs were obtained following the removal of Cellhesion®. It is important to note that while this method does not guarantee complete material removal, the residual amount is minimal (Fig. 3A–C). Importantly, this residual material is not expected to significantly affect the comparison of proliferation rates in traditional culture conditions. The UCMSCs, after the elution, were subjected to a comparative assessment with 2D culture UCMSCs to evaluate their proliferation capacity. 2D and 3D UCMSCs were seeded at a density of 1×10^5 cells/ml in culture dishes with adhesive properties, and their numbers were quantified daily using embryonic blue staining. On day three of proliferation, the average cell count for the 2D culture was 2.68×10^5, while that for the 3D culture was 8.04×10^5. The 3D group exhibited a substantial advantage, approximately twofold higher than the 2D group. This advantage persisted throughout the culture period, with cells continuing to proliferate exponentially. On day five, the average cell count for the 2D culture was 4.49×10^5, whereas that for the 3D culture was 6.27×10^5. Limited by the petri dish area size, the 3D group peaked on the fourth day. Although the 3D proliferation rate slightly declined, from 9.781×10^5 On day four (Fig. 3E), it outperformed the traditional culture method. These findings collectively indicate that UCMSCs cultured in the presence of Cellhesion® exhibit a higher proliferation rate and enhanced proliferation capacity.

3.4. Identification of 3D cultured UCMSCs

Evaluating three differentiation capabilities and cell surface antigen markers serves as crucial criteria for characterizing umbilical cord stem cells [20]. We conducted a comparative validation of UCMSCs cultured in traditional 2D conditions and those subjected to a 3D culture, using three differentiation assays. These experiments, encompassing lipogenic, osteogenic, and chondrogenic differentiation, were performed concurrently, yielding consistent results (Fig. 4A).

Expression of stem cell markers on UCMSCs cultured in a 3D environment: As MSCs are known to express CD90, CD73, and CD105 antibodies while lacking CD11b, CD19, CD34, CD45, and HLA-DR markers, we confirmed these cell surface antigen markers through flow cytometry experiments. These experiments were conducted on UCMSCs from the same batch and generation that underwent proliferation assays (Fig. 4B). The outcomes demonstrate that UCMSCs following Cellhesion® 3D culture retained the fundamental characteristics of stem cells and exhibited no alterations in their stem cell phenotype.

3.5. Paracrine factors from UCMSCs with Cellhesion®

The analysis of paracrine factor secretion from UCMSCs after 3D culture was contrasted with that from 2D culture using an ELISA kit. Four representative paracrine factors, namely hepatocyte growth factor (HGF), vascular endothelial growth factor (VEGF), interleukin-6 (IL-6), and interleukin-8 (IL-8), were selected to assess the enhanced paracrine activity facilitated by Cellhesion®, focusing on factors associated with tissue regeneration and inflammation regulation (Fig. 5A).

Cytokine profiling of UCMSCs in 3D culture: In the comparison between HGF and VEGF, the 3D group displayed a significant advantage, with an exponential increase in VEGF paracrine concentration observed from the second day of culture, maintaining this advantage throughout the proliferative culture period. Conversely, when comparing IL-6, the 3D group did not exhibit an absolute advantage in the early stages but demonstrated a pronounced advantage in the later stages of culture. Similarly, for IL-8, the 3D group demonstrated an initial advantage and underwent exponential growth by the end of the culture cycle. VEGF served as a valuable vascular endothelial growth factor in the above findings. At the same time, we simultaneously conducted angiogenesis experiments (Fig. 5B). The analysis of angiogenesis results after 20 h, using ImageJ software, indicated that the lumen length formed in the 3D group was greater than that in the 2D group. Both in terms of the quantity and length of angiogenesis, 3D culture exhibited a substantial advantage.

3.6. UCMSCs paracrine secretion and angiogenesis

In the vascular experiment, vascular morphogenesis was observed in all experimental groups except for the MSC culture medium group at the 12-h time point (Fig. 5B). Following this initial observation, there were

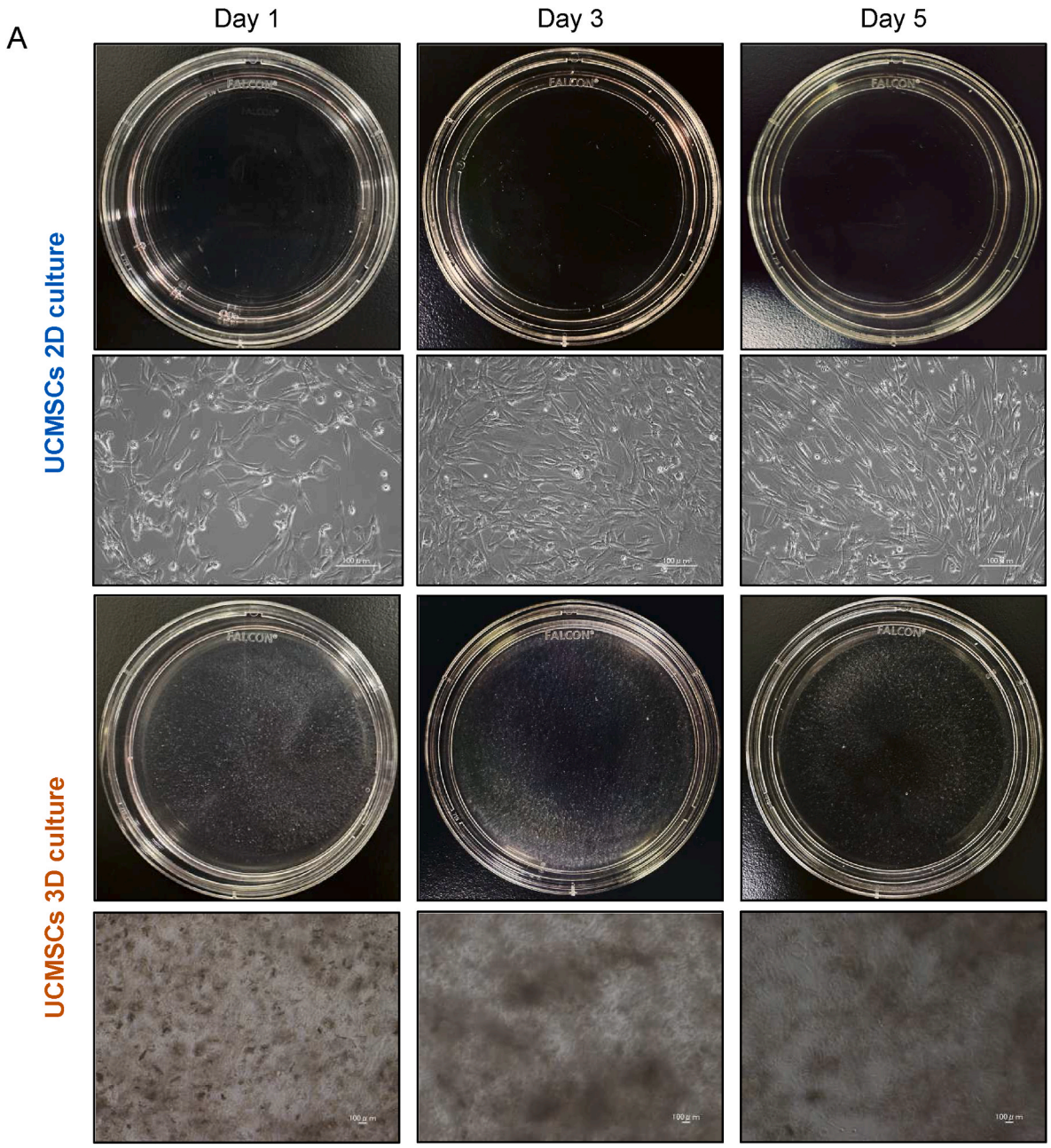

Fig. 2. The cell proliferation assay with Cellhesion® culture. (A) The study involved observing the 2D and 3D UCMSC cultures on days 1, 3, and 5, with the naked eye and under a microscope at 10 × magnification. The 3D group showed the presence of white flocculent material and cells when observed with the naked eye and clusters under a 10 × microscope. (B) Growth comparison between 2D-vs. 3D-cultured UCMSCs. Plots indicate mean ± SEM (n = 3). Cell counting was performed using embryonic blue staining on 2D and 3D cultures to measure cell proliferation within five days.

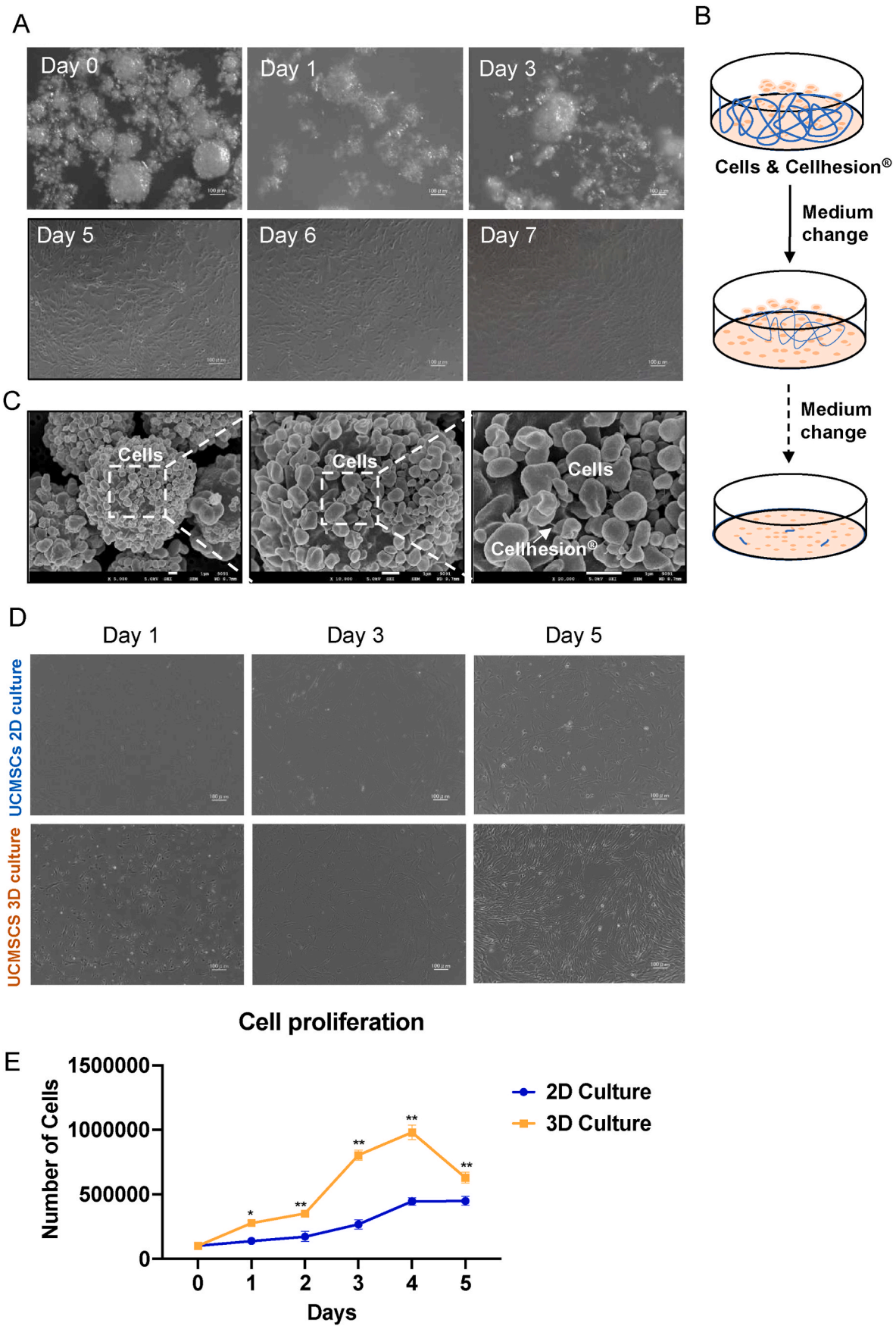

(caption on next page)

Fig. 3. Removal of UCMSCs from Cellhesion® (A) Cells with Cellhesion® were seeded in a 2D culture dish and added to the culture medium. After 24 h, the cells gradually moved out of Cellhesion®, and the Cellhesion® was washed away gradually every three days with the medium change. With the number of replacements, it was clear that there was much less Cellhesion® on Day 3, and almost none on Day 5 and Day 7. (B) The Cellhesion® flowchart. (C) Observation of the cells' removal from Cellhesion® under scanning electron microscopy at 5000 × , 10,000 × , and 20,000 × . Tiny residues of Cellhesion® could be seen when magnified to 20,000 × . (D) The cell proliferation of UCMSCs in 2D and 3D cultures was measured by counting the cells using embryonic blue staining after removing Cellhesion® within five days. (E) Growth comparison between 2D-vs. 3D-cultured UCMSCs extracted from the 3D material. Plots indicate mean ± SEM (n = 3). Cell counting was performed on 2D and 3D cultures to measure cell proliferation within five days.

no further alterations in vascular morphology over time. Using ImageJ software for quantitative analysis, the length of vascular structures in the 3D group measured 4093.702 units, whereas in the 2D group, it was 1395.065 units. The vascular length in the HUVEC culture medium group was 866.912 units, while no vascular structure formation in the MSC group could be detected. These results underscore the significant advantage of the 3D group, with luminal structure length being more than twice that of the 2D group. These findings affirm that the 3D culture environment, particularly when employing Cellhesion®, confers a notable advantage in the production of VEGF. This enhancement in VEGF production likely contributes to the observed improvements in vascular morphogenesis.

3.7. Colony forming units

The colony formation assay is a robust methodology commonly employed in current *in vitro* experiments involving hematopoietic stem cells. By quantifying the number of culture well plates in which colonies formed, out of a total of 60 well plates, the results yielded an average of 22 well plates in the 2D group and 29 well plates in the 3D group (Fig. 5C). These findings strongly support the conclusion that UCMSCs cultured with Cellhesion® possess an enhanced ability to form colonies, indicative of their heightened proliferative potential [28,29].

3.8. RNA sequencing of 2D and 3D cultured UCMSCs

To gain deeper insights into the distinctions between UCMSCs cultivated under the two different culture conditions, RNA sequencing was performed on passages of four UCMSCs cultured either in a 2D or 3D medium (Fig. 6B). Gene ontology (GO) (Fig. 6C) enrichment analysis revealed that the differentially expressed genes were primarily enriched in pathways related to anti-inflammation, DNA repair, cell cycle regulation, DNA replication, proliferation, the minichromosome maintenance (MCM) complex, and other processes associated with cell proliferation. Furthermore, the enrichment analysis also indicated terms related to molecular binding events pertinent to intercellular signaling processes. Additionally, noteworthy observations included the downregulation of KLF4 among the differentially expressed genes, suggesting a potential role in augmenting stemness under 3D culture conditions. Simultaneously, an upregulation of CXCL12 was noted, which facilitates MSCs in inducing M1-type polarization of macrophages [30]. This implies a role for CXCL12 in the resolution of inflammatory processes, underscoring the multifaceted effects of 3D culture on UCMSCs (Fig. 6A).

4. Discussion

This study sought to reveal the effects of chitin nanocomposite 3D scaffolds on achieving cell properties through biomaterial-cell dynamics in early culture, including proliferation and stemness maintenance, constructing an artificial microenvironment strategy suitable for high-quality *in vitro* culture of UCMSCs to achieve quality control (Table 1). This system will provide a bridge for therapies based on MSCs and derived or auxiliary products to move from basics to clinical application [31]. It has been reported that the heterogeneity and loss of stemness caused by the over-expansion of adipose MSC *in vitro* can be reduced by non-adherent cultures of chitosan microspheres [32]. Similar to the microsphere scaffold, in this study, human UCMSCs achieved a semi-floating state when supported and surrounded by a chitin matrix, forming a dynamic interactive artificial niche and slowing down the expansion behavior of UCMSCs. With the replacement of the cell culture medium, the chitin scaffold matrix is rapidly cleared, causing the UCMSC culture to transition from 3D to 2D, leading to a swift increase in the proliferation rate of UCMSCs. This change in cell proliferation in 3D culture is consistent with the known universal plasticity of MSCs [33]. It once again verifies the widely variable regulation of stem cell programs by physiological microenvironment simulation [34]. It can be seen that the MSC stemness maintenance ability produced by Cellhesion® has certain spatiotemporal properties similar to those *in vivo*, such as potentially greatly expanding the bioavailability of chitin [35–37].

In the early stages of 3D culture, the interactive deposition of chitin and cells may be a rapid biological process related to the chitin skeleton's stability at the microscale [37] and increased biodegradation [38]. Long-term *in vitro* 3D culture of mammalian MSCs may reduce treatment safety and efficiency [39], while 3D scaffold-assisted culture systems may improve it [40]. Although we created a 3D culture model of UCMSCs in a petri dish through chitin fiber doping, Cellhesion® UCMSCs are not fully biodegradable due to the different biodegradation of chitin *in vivo* [41], coupled with the potential immunogenicity of chitin and its metabolites [42]. Their suitability for direct transplantation is unknown. It is worth noting that transplantable or injectable hybrid nanoscaffolds facilitate the rapid assembly, improved survival rate, and maintenance of stemness of stem cells in the body, while cellulose cryogel reinforced with chitin nanowhiskers exhibits better performance in terms of biocompatibility, compared to MSCs [43]. Therefore, biodegradable nanochitin carriers may be expected to assemble functional UCMSCs through synergistic 3D cell-cell and cell-matrix interactions, thereby creating a favorable physical microenvironment for UCMSC delivery *in vivo* and expanding their scope of application [44,45].

While maintaining stemness, UCMSCs can have biological interactive communication with the 3D culture microenvironment through their unique paracrine effects [46]. This is also the biological basis for MSC transplantation therapy to produce tissue regeneration, repair, and immune regulation. This study shows that UCMSCs cultured in 3D exhibited increased functional exocrine levels compared with continuous 2D culture, suggesting that the 3D microenvironment stimulates additional useful cellular pathways. Earlier studies reported that UCMSCs based on rotational 3D culture could achieve complete wound healing in rats, with a higher degree of vascularization, by activating higher levels of functional secretome while maintaining stem cell identity markers [47]. Since MSC paracrine-mediated immune regulation may have significant tissue specificity [48] and niche response changes [49], the short-term microenvironmental modification formed by Cellhesion® culture simulates the plasticity of UCMSC secretory behavior to a certain extent. In addition, recent studies have suggested that UCMSC exocrine vesicles alone have biological carrier properties and can be designed to deliver therapeutic biological macromolecules efficiently *in vivo* [50]. On the other hand, engineered chitosan (the *in vivo* deacetylation product of chitin) nanoparticles were found to promote the *in vivo* repair of fibroblasts by modulating a specific inflammatory microenvironment and reprogramming the proteome and cytokine profile of macrophages [51]. This jointly suggests that Cellhesion® UCMSCs can potentially enrich the exocrine effects of MSCs after transplantation, providing a new intersection of biology and materials for further exploration of cell therapy based on the unique

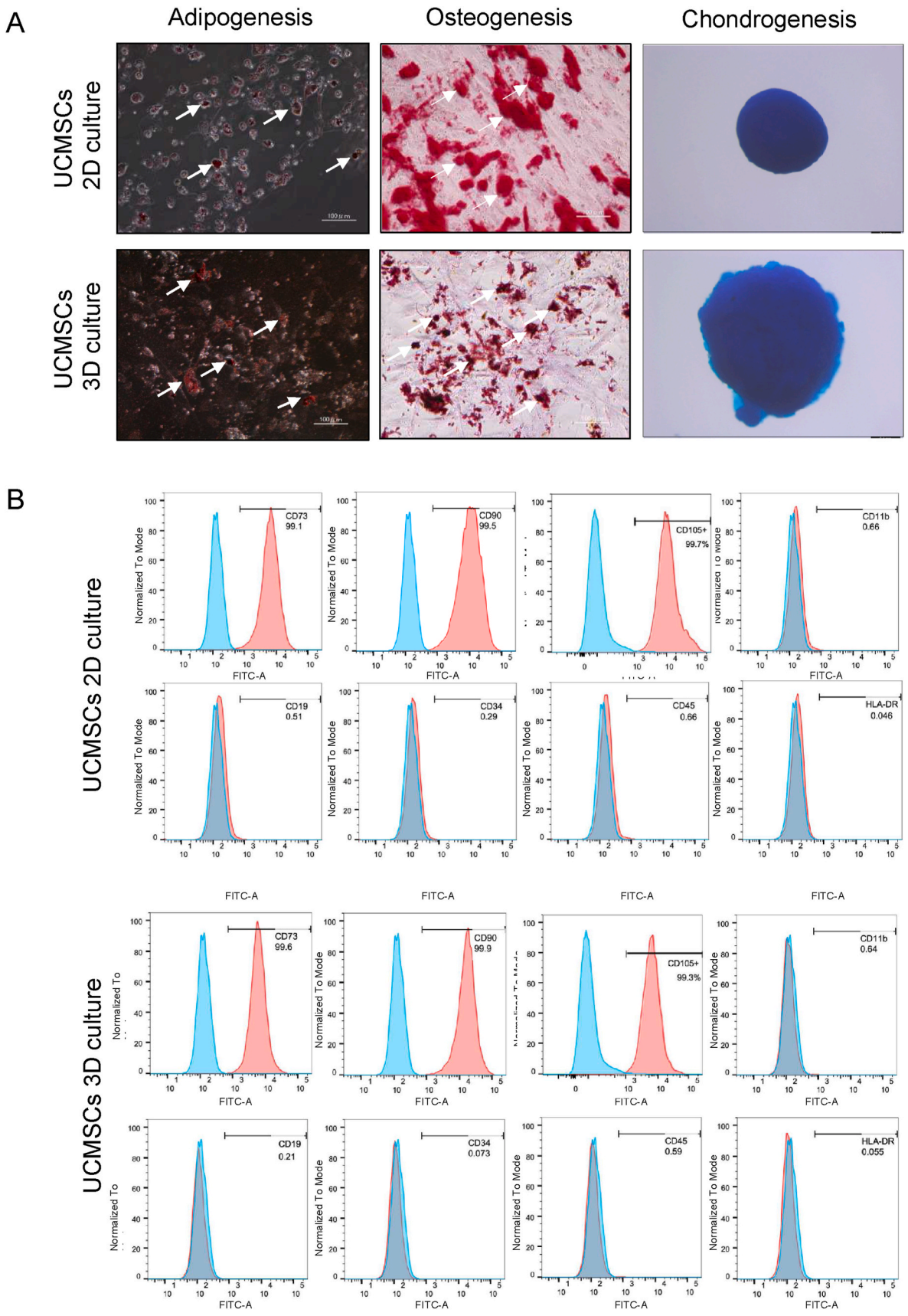

Fig. 4. Cell characteristic tests of 2D and 3D culture UCMSCs. (A) The results show the differentiation of UCMSCs into lipogenic, osteogenic, and chondrogenic tissues in both the 2D and 3D groups. The white arrows represent the cells that have been stained for osteogenesis and adipogenesis. (B) Flow cytometric analysis of stemness markers; positive cell populations in 2D and 3D culture cells. The results show that CD73, CD90, and CD105 are positively expressed in both groups, while CD11b, CD19, CD34, CD45, and HLA-DR are negatively expressed.

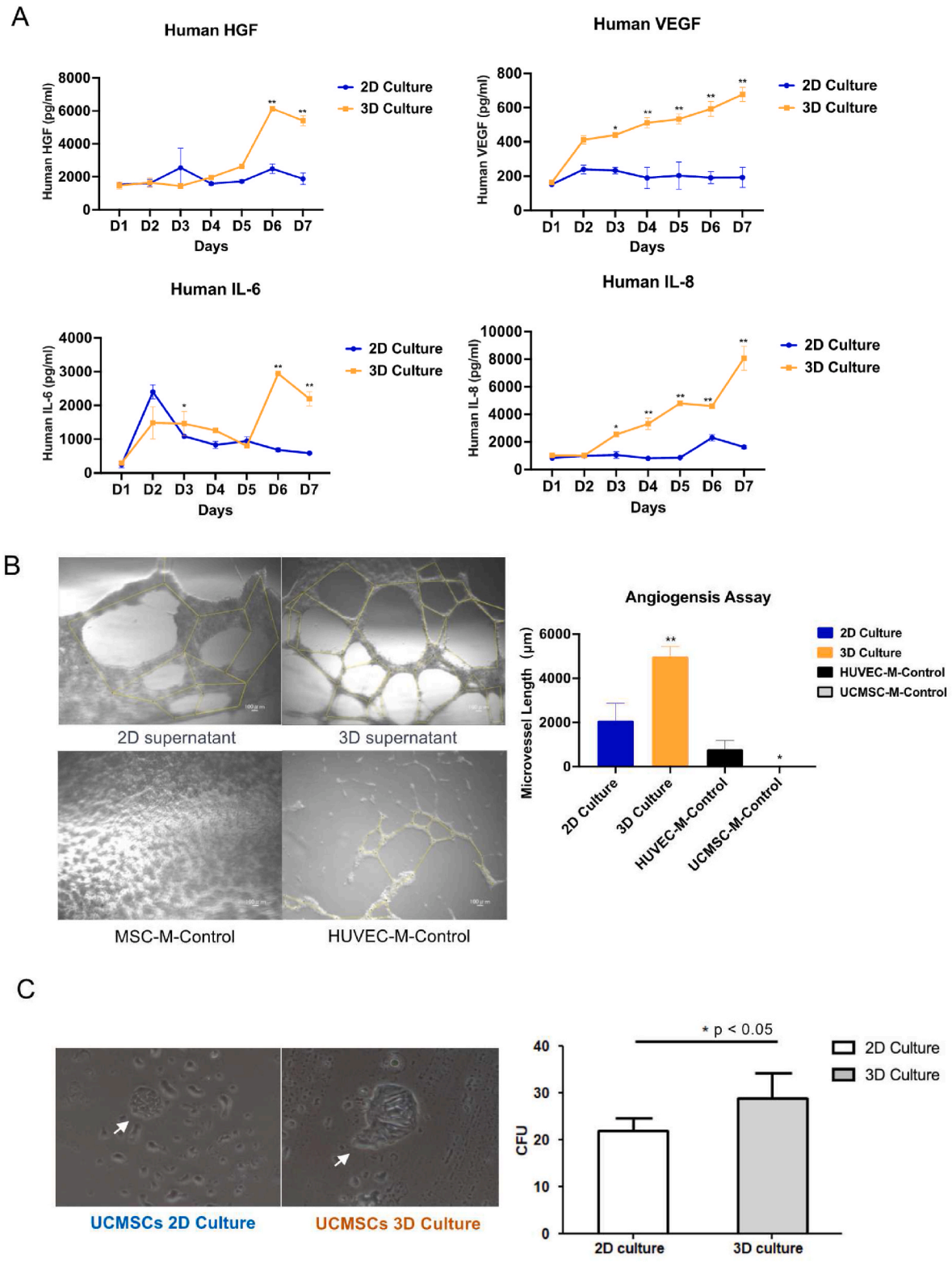

Fig. 5. Paracrine effects, angiogenesis, and CFU assay results of MSCs cultured in 2D and 3D. (A) An Elisa assay tested the paracrine amounts of HGF, VEGF, IL-6, and IL-8 in the 2D and 3D cultures daily for seven days. The Y-axis is the factor concentration and the X-axis is the number of days in time. Bars indicate mean ± SD. **p < 0.01, *p < 0.05 (B) Angiogenesis experiments were conducted on HUVEC using the supernatant from the 2D group (blue plot with a column), 3D group UCMSCs (orange plot with a column), and HUVEC (black plot with a column), MSC culture medium in the gel. The final vascularization condition and the length of the formed vessels were noted. Bars indicate mean ± SEM (n = 3). (C) Results of the colony-forming unit (CFU) assay for both the 2D and 3D groups. The left panel on the figure shows an enlarged view of single-cell expansion (20× microscope magnification). The right panel on the figure illustrates the growth comparison between 2D and retrieved cells of 3D-cultured h-MSCs. Bars represent mean ± SD (n = 3), *p < 0.05.

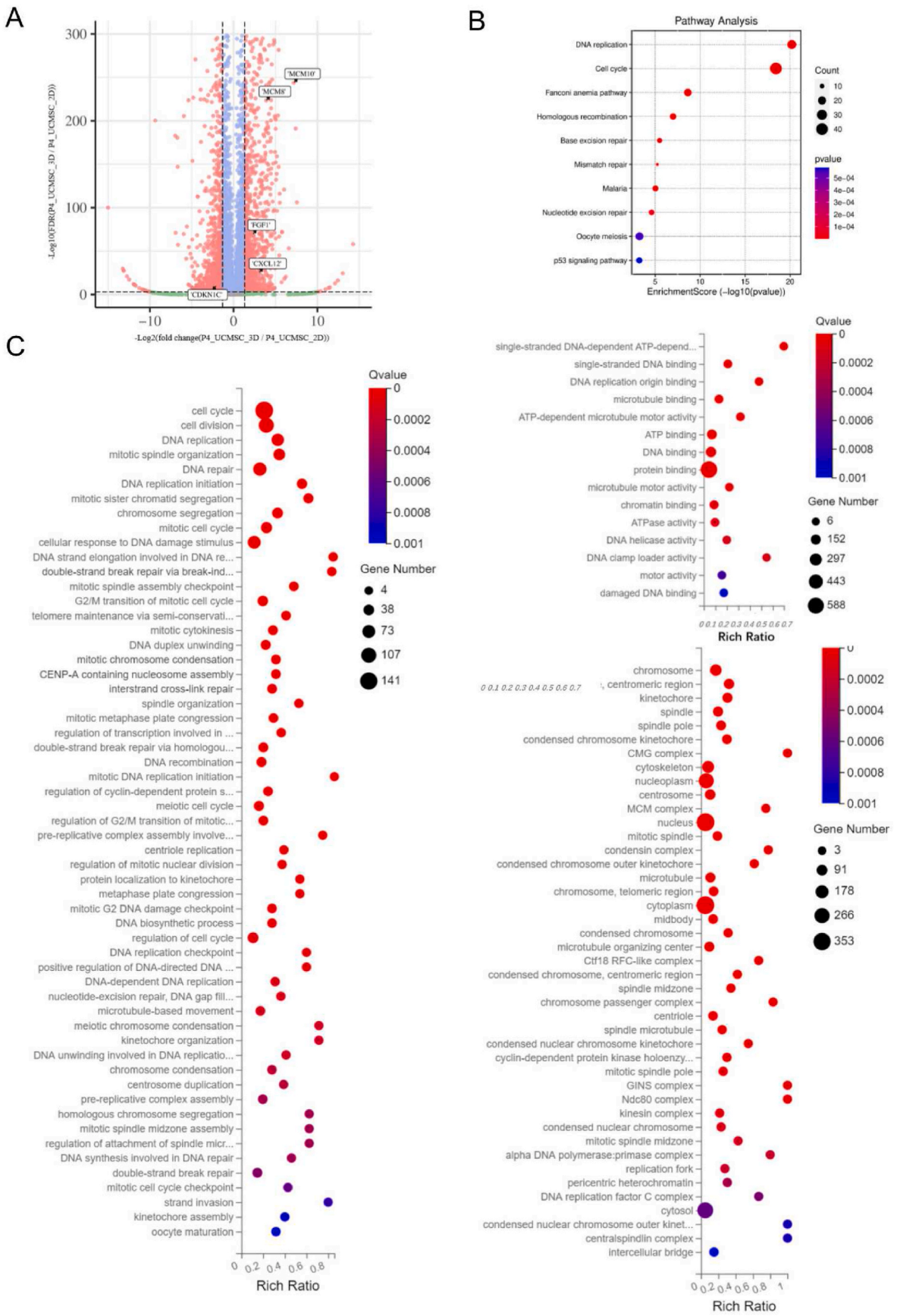

(caption on next page)

Fig. 6. (A, B, C) Replicate RNA-seq libraries were prepared from UCMSCs cultured in 2D and 3D. The sequencing data was filtered with SOAP nuke (v1.5.6) by removing adopter reads, low-quality reads, and reads whose unknown base ('N' base) ratio was more than 5 %. Clean reads were obtained, stored in FASTQ format, and mapped to the reference genome using HISAT2 (v2.1.0). Bowtie2 (v2.3.4.3) was applied to align the clean reads to the gene set. RSEM (v1.3.1) calculated the expression level of the gene. The heatmap was generated by pheatmap (v1.0.8). Differential expression analysis was performed using the DESeq2 (v1.4.5) with $|\log2FC| \geq 2.5$, FDR ≤ 0.001, and visualized by an enhanced volcano (v3.16). GO (http://www.geneontology.org/) and Phyper performed KEGG (https://www.kegg.jp/) enrichment analysis of annotated different expression genes based on the hypergeometric test. The significant levels of terms and pathways were corrected by Q value with a rigorous threshold (Q value ≤ 0.05).

Table 1
Comparison of 2D and 3D UCMSC culture methods.

Main Features	2D Cell Culture	3D Cell Culture
Cell shape	Flat and stretched	Natural cell shape is preserved.
Cell polarity is present	Contact between cells and culture medium.	There is a gradient in the concentration of medium components surrounding the cells similar to the physiological environment.
Intercellular connections	A low percentage of intercellular connections could be found.	Intercellular connections are abundant, allowing for effective intercellular communication.
Cellular differentiation	Differentiation into bone, lipids, and cartilage is maintained.	Differentiation into bone, lipids, and cartilage is maintained.
UCMSC markers	CD73, CD90, CD105, CD11b, CD19, CD34, CD45, HLA-DR	CD73, CD90, CD105, CD11b, CD19, CD34, CD45, HLA-DR
mRNA expression	OCT4, NANOG, CXCR4	Higher levels of OCT4, NANOG, CXCR4
Cell proliferation	Cells are proliferating.	In the same conditions, the rate of cell proliferation is higher.
Paracrine Factors	HGF, VEGF, IL-6, IL-8	In the same conditions, HGF, VEGF, IL-6, and IL-8 levels also increased and became more pronounced.
Angiogenesis	Luminal area, total lengthening, and number of branching points were observed.	There were a greater number of lumen areas, increased lengthening, and more branching points.

UCMSC Umbilical cord mesenchymal stem cell, HGF Hepatocyte growth factor, VEGF Vascular endothelial growth factor.
UCMSC markers are positive for CD105, CD90 and CD73, and negative for CD11b, CD34, CD45, and HLA-DR.

biological activity of UCMSCs. In terms of biomaterial safety, Chitin, a long-chain polymer of N-acetylglucosamine has been used as a scaffold in studies of tissue growth and wound healing, so Cellhesion® by chitin is more natural and provides a biosafety advantage in the applications.

The compliance changes in UCMSC gene expression profiles caused by 3D culture based on the auxiliary properties of active biomaterials are an important quality control indicator for the future clinical transformation of UCMSC and a potential key basis for the continuous improvement of cell transplantation therapy [52]. It has been reported that the nuclei of MSCs cultured on 3D biological scaffolds are rounder than those cultured in 2D and are accompanied by a uniform distribution of euchromatin, leading to gene expression fluctuations [53]. The RNA-seq results here show that, compared with 2D culture, the gene expression differences created by Cellhesion® are mainly due to the enhancement of the fidelity replication process of DNA and may also be related to the increased responsiveness of active chromatin. Our research results indicate that UCMSC cultured in 3D significantly alters higher-order genomic interactions, which may be consequential for the subset of genes that are important for the physiological functioning of the cells. To a certain extent, the 3D adaptability of the transcription machinery in the nucleus explains the power source of UCMSC proliferation and paracrine enhancement. With the unexpected drift of gene expression profiles, UCMSCs in the bionic microenvironment exhibit obvious pluripotency characteristics and reproduce active self-renewal capabilities. Therefore, Cellhesion®-mediated stemness enhancement undoubtedly positively affects the regeneration and repair of transplanted UCMSCs *in vivo*. Of course, since overactive DNA replication and transcription may cause genetic and epigenetic changes, the safety of this additional genomic push requires further study to avoid non-functional subtype transitions in UCMSCs [54].

With the foundational methodologies of *in vitro* cultivation using Cellhesion MSCs, MSCs can produce enhanced quality cell supernatant therapeutic fluids and exosomes for clinical interventions such as tissue regeneration, vascular repair, and anti-inflammatory treatments. Additionally, there is the potential to fabricate consistent, high-quality single-cell products suitable for pharmaceutical research and related domains. On another note, in applications with lower material sensitivity, there is the prospect of venturing into cartilage regeneration and the production processes of tissue engineering products (Fig. 7). This provides a robust research foundation and underscores the untapped potential for industrial production and clinical application of *in vitro* MSCs. However, like this study, 3D culture methods using biocompatibility and biodegradability still have limitations. First, compared with traditional 2D culture methods, stable 3D culture methods require relatively more complex biological technologies, including initial cell affinity micro-scaffolds, cell seeding, and fine control of culture conditions. Secondly, since the establishment and remodeling of the 3D matrix is dynamic, the starting materials must have stiffness, viscoelasticity, and degradability characteristics as close as possible to the native tissue, and their physical and chemical properties must be fully evaluated. Although advanced 3D culture can improve the *in vitro* biological activity of UCMSCs, achieving final clinical transformation may require further exploration of cell loading strategy optimization, the addition of appropriate active factors, preclinical animal experiments, and molecular mechanisms. Since the goal of 3D culture is to progress toward clinical applications, animal experiments are a crucial step in a preclinical study. We are planning to conduct experiments that include models for myocardial ischemia, limb ischemia, and knee joints to evaluate the safety and effectiveness after MSC transplantation. On the other hand, Another important aspect to consider is the comparison of Cellhesion® with other 3D culture materials. such as hydrogels, high molecular weight polyethylene, and other 3D materials in our further studies.

5. Conclusion

A 3D culture method using Cellhesion® enabled UCMSCs to increase cellular proliferation and enhance both the inherent stemness of the cells and the paracrine secretion capabilities of MSCs. Subsequent cellular and biochemical assays highlighted a notable upregulation in CXCL12, MCM8, and MCM10 expression levels, further strengthening the cells' ability to promote angiogenesis. These data support the potential application of Cellhesion® as a therapeutic agent under these specific conditions. This investigation provides foundational insights for anticipating clinical applications centered on paracrine secretion, inflammatory cytokine release, and stem cell clonal development proficiency. Consequently, we advocate incorporating Cellhesion® as a matrix in 3D cultivation strategies or as an essential component in tissue engineering endeavors. Such an approach holds considerable promise for amplifying the efficacy and scalability of MSCs, thereby rendering them advantageous in clinical mesenchymal stem cell applications.

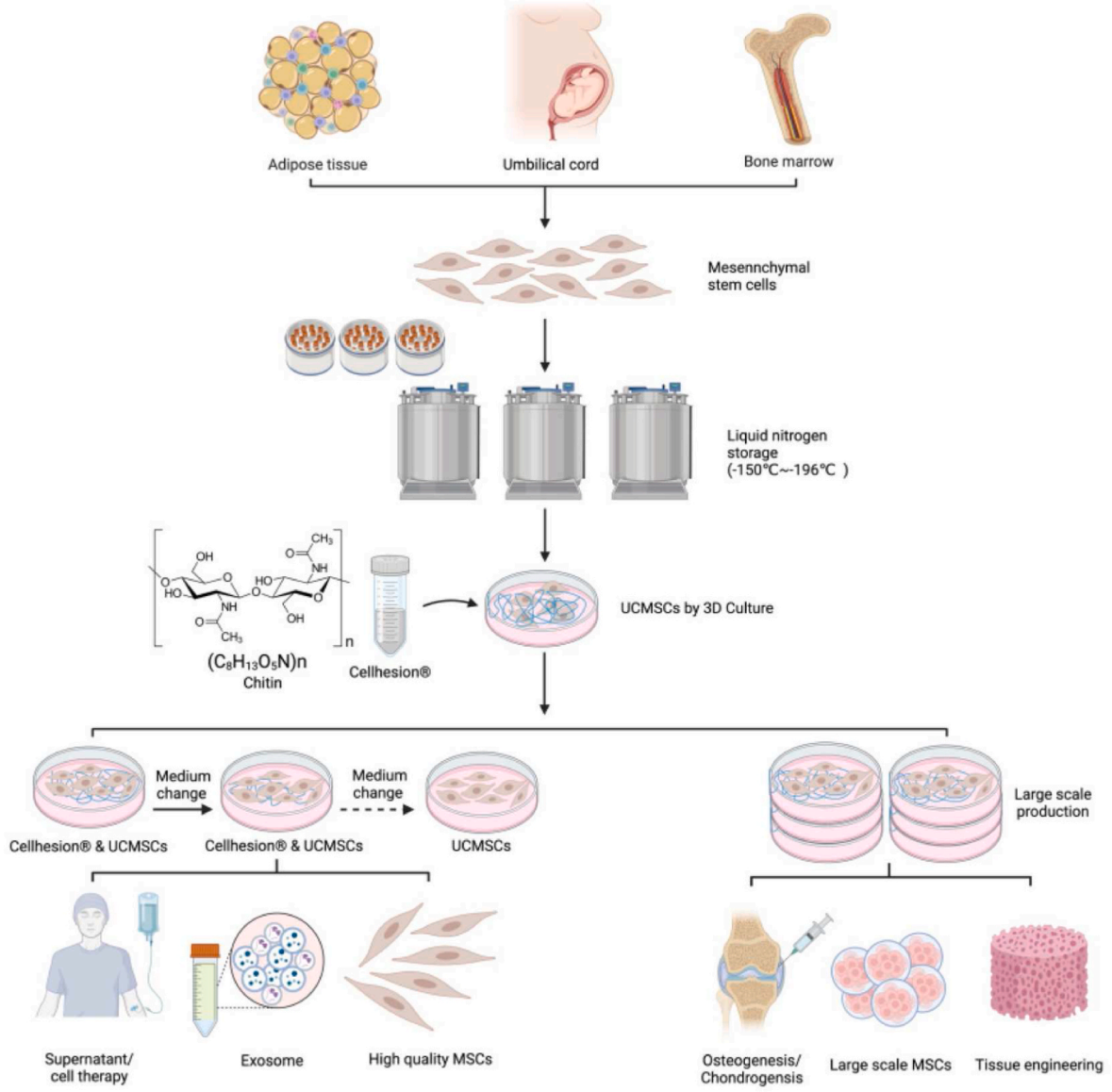

Fig. 7. Cellhesion® is an important component in the cultivation and nurturing stages of adipose, umbilical, and bone marrow-derived MSCs. It helps in cultivating cells with enhanced proliferation and paracrine abilities. Once Cellhesion® is removed, the enhanced MSCs can be used for cell therapy, producing high-quality exosomes and MSCs. Moreover, when they contain Cellhesion®, these enhanced MSCs can be used for cartilage regeneration, tissue engineering, and mass culture of cells.

Funding

Not applicable.

Availability of data and materials

The authors will provide the original data supporting the conclusions of this paper without reservation.

Declarations

The authors declare that the study was conducted without any business or financial relationships that could be interpreted as potential conflicts of interest.

Ethics approval and consent to participate

All procedures in this study were performed following the regulations of the Ethics Committee or Institutional Review Board.

Consent to publication

Not applicable.

CRediT authorship contribution statement

Shuoji Zhu: Writing – original draft, Formal analysis, Data curation. **Junfeng Xuan:** Software, Formal analysis, Data curation. **Yunchao Shentu:** Writing – original draft, Software, Formal analysis, Data curation. **Katsuhiko Kida:** Formal analysis, Data curation. **Masaki Kobayashi:** Methodology, Formal analysis. **Wei Wang:** Resources, Conceptualization. **Minoru Ono:** Writing – review & editing, Conceptualization. **Dehua Chang:** Writing – review & editing, Project administration, Methodology, Formal analysis, Data curation, Conceptualization.

Declaration of competing interest

The authors declare no conflict of interest.

Acknowledgements

This study's experimental data analysis received support in the review from Juan Wang Shuang Gao and Zhixin Zhang in BOE Regenerative Medicine Technology Co., Ltd.

Flow cytometric data acquisition received support from Myoji Watanabe in the One-stop Sharing Facility Center for Future Drug Discoveries at the Graduate School of Pharmaceutical Sciences, University of Tokyo.

Appendix A. Supplementary data

Supplementary data to this article can be found online at https://doi.org/10.1016/j.bioactmat.2024.01.014.

References

[1] A. Uccelli, L. Moretta, V. Pistoia, Mesenchymal stem cells in health and disease, Nat. Rev. Immunol. 8 (9) (2008) 726–736, https://doi.org/10.1038/nri2395.
[2] T. Squillaro, G. Peluso, U. Galderisi, Clinical trials with mesenchymal stem cells: an update, Cell Transplant. 25 (5) (2016) 829–848, https://doi.org/10.3727/096368915X689622.
[3] L. Li, Y. Zhang, J. Mu, J. Chen, C. Zhang, H. Cao, J. Gao, Transplantation of human mesenchymal stem-cell-derived exosomes immobilized in an adhesive hydrogel for effective treatment of spinal cord injury, Nano Lett. 20 (6) (2020) 4298–4305, https://doi.org/10.1021/acs.nanolett.0c00929.
[4] C.M. Dunn, S. Kameishi, D.W. Grainger, T. Okano, Strategies to address mesenchymal stem/stromal cell heterogeneity in immunomodulatory profiles to improve cell-based therapies, Acta Biomater. 133 (1) (2021) 114–125, https://doi.org/10.1016/j.actbio.2021.03.069.
[5] S. Regmi, S. Pathak, J.O. Kim, C.S. Yong, J.H. Jeong, Mesenchymal stem cell therapy for the treatment of inflammatory diseases: challenges, opportunities, and future perspectives, Eur. J. Cell Biol. 98 (5–8) (2019) 151041, https://doi.org/10.1016/j.ejcb.2019.04.002.
[6] S.J. Morrison, A.C. Spradling, Stem cells and niches: mechanisms that promote stem cell mainte1nance throughout life, Cell 132 (4) (2008) 598–611, https://doi.org/10.1016/j.cell.2008.01.038.
[7] D.T. Scadden, Nice neighborhood: emerging concepts of the stem cell niche, Cell 157 (1) (2014) 41–50, https://doi.org/10.1016/j.cell.2014.02.013.
[8] H. Liang, Y. Ao, W. Li, K. Liang, B. Tang, J. Li, J. Wang, X. Zhu, Y. Du, Injectable bone marrow microniches by co-culture of HSPCs with MSCs in 3D microscaffolds promote hematopoietic reconstitution from acute lethal radiation, Bioact. Mater. 22 (2022) 453–465, https://doi.org/10.1016/j.bioactmat.2022.10.015.
[9] S. Zhu, C. Yu, N. Liu, M. Zhao, Z. Chen, J. Liu, G. Li, H. Huang, H. Guo, T. Sun, J. Chen, J. Zhuang, P. Zhu, Injectable conductive gelatin methacrylate/oxidized dextran hydrogel encapsulating umbilical cord mesenchymal stem cells for myocardial infarction treatment, Bioact. Mater. 13 (2021) 119–134, https://doi.org/10.1016/j.bioactmat.2021.11.011.
[1][0] L.L. Lu, Y.J. Liu, S.G. Yang, Q.J. Zhao, X. Wang, W. Gong, Z.B. Han, Z.S. Xu, Y. X. Lu, D. Liu, Z.Z. Chen, Z.C. Han, Isolation and characterization of human umbilical cord mesenchymal stem cells with hematopoiesis-supportive function and other potentials, Haematologica 91 (8) (2006) 1017–1026. Epub2006Jul25.
[11] D.C. Ding, Y.H. Chang, W.C. Shyu, S.Z. Lin, Human umbilical cord mesenchymal stem cells: a new era for stem cell therapy, Cell Transplant. 24 (3) (2015) 339–347, https://doi.org/10.3727/096368915X686841.
[12] T. Xin, V. Greco, P. Myung, Hardwiring stem cell communication through tissue structure, Cell 164 (6) (2016) 1212–1225, https://doi.org/10.1016/j.cell.2016.02.041.
[13] D. Xing, W. Liu, J. Li, L. Liu, A. Guo, B. Wang, H. Yu, Y. Zhao, Y. Chen, Z. You, C. Lyu, W. Li, A. Liu, Y. Du, J. Lin, Engineering 3D functional tissue constructs using self-assembling cell-laden microniches, Acta Biomater. 15 (114) (2020) 170–182, https://doi.org/10.1016/j.actbio.2020.07.058.
[14] E. Cesare, A. Urciuolo, H.T. Stuart, E. Torchio, A. Gesualdo, C. Laterza, O. Gagliano, S. Martewicz, M. Cui, A. Manfredi, L. Di Filippo, P. Sabatelli, S. Squarzoni, I. Zorzan, R.M. Betto, G. Martello, D. Cacchiarelli, C. Luni, N. Elvassore, 3D ECM-rich environment sustains the identity of naive human iPSCs, Cell Stem Cell 29 (12) (2022) 1703–1717.e7, https://doi.org/10.1016/j.stem.2022.11.011.
[15] C. Li, G. Li, M. Liu, T. Zhou, H. Zhou, Paracrine effect of inflammatory cytokine-activated bone marrow mesenchymal stem cells and its role in osteoblast function, J. Biosci. Bioeng. 121 (2) (2016) 213–219, https://doi.org/10.1016/j.jbiosc.2015.05.017.
[16] T.H. Ambrosi, O. Marecic, A. McArdle, R. Sinha, G.S. Gulati, X. Tong, Y. Wang, H. M. Steininger, M.Y. Hoover, L.S. Koepke, M.P. Murphy, J. Sokol, E.Y. Seo, R. Tevlin, M. Lopez, R.E. Brewer, S. Mascharak, L. Lu, O. Ajanaku, S.D. Conley, J. Seita, M. Morri, N.F. Neff, D. Sahoo, F. Yang, I.L. Weissman, M.T. Longaker, C.K. F. Chan, Aged skeletal stem cells generate an inflammatory degenerative niche, Nature 597 (7875) (2021) 256–262, https://doi.org/10.1038/s41586-021-03795-7.
[17] Q. Sun, W. Lee, H. Hu, T. Ogawa, S. De Leon, I. Katehis, C.H. Lim, M. Takeo, M. Cammer, M.M. Taketo, D.L. Gay, S.E. Millar, M. Ito, Dedifferentiation maintains melanocyte stem cells in a dynamic niche, Nature 16 (7958) (2023) 774–782, https://doi.org/10.1038/s41586-023-05960-6.
[18] L. Xin, X. Lin, F. Zhou, C. Li, X. Wang, H. Yu, Y. Pan, H. Fei, L. Ma, S. Zhang, A scaffold laden with mesenchymal stem cell-derived exosomes for promoting endometrium regeneration and fertility restoration through macrophage immunomodulation, Acta Biomater. 1 (113) (2020) 252–266, https://doi.org/10.1016/j.actbio.2020.06.029.
[19] Y. Qiao, Z. Xu, Y. Yu, S. Hou, J. Geng, T. Xiao, Y. Liang, Q. Dong, Y. Mei, B. Wang, H. Qiao, J. Dai, G. Suo, Single cell derived spheres of umbilical cord mesenchymal stem cells enhance cell stemness properties, survival ability and therapeutic potential on liver failure, Biomaterials 227 (2020) 119573, https://doi.org/10.1016/j.biomaterials.2019.119573.
[20] L. Fu, P. Li, J. Wu, Y. Zheng, C. Ning, Z. Liao, X. Yuan, Z. Ding, Z. Zhang, X. Sui, S. Shi, S. Liu, Q. Guo, Tetrahedral framework nucleic acids enhance the chondrogenic potential of human umbilical cord mesenchymal stem cells via the PI3K/AKT axis, Regen. Biomater. (2023) 10, https://doi.org/10.1093/rb/rbad085.
[21] S. Keshtkar, N. Azarpira, M.H. Ghahremani, Mesenchymal stem cell-derived extracellular vesicles: novel frontiers in regenerative medicine, Stem Cell Res. Ther. 9 (1) (2018) 63, https://doi.org/10.1186/s13287-018-0791-7.
[22] I. Majore, P. Moretti, R. Hass, C. Kasper, Identification of subpopulations in mesenchymal stem cell-like cultures from human umbilical cord, Cell Commun. Signal.: CCS 7 (2009) 6, https://doi.org/10.1186/1478-811X-7-6.
[23] Z. Wang, C. Chai, R. Wang, Y. Feng, L. Huang, Y. Zhang, X. Xiao, S. Yang, Y. Zhang, X. Zhang, Single-cell transcriptome atlas of human mesenchymal stem cells exploring cellular heterogeneity, Clin. Transl. Med. 11 (12) (2021) e650, https://doi.org/10.1002/ctm2.650.
[24] T. Nagamura-Inoue, T. Mukai, Umbilical cord is a rich source of mesenchymal stromal cells for cell therapy, Curr. Stem Cell Res. Ther. 11 (8) (2016) 634–642, https://doi.org/10.2174/1574888x10666151026115017.
[25] E.S. Kim, K. Kida, J. Mok, Y. Seong, S.Y. Jo, T. Kanaki, M. Horikawa, K.H. Kim, T. M. Kim, T.S. Park, J. Park, Cellhesion VP enhances the immunomodulating potential of human mesenchymal stem cell-derived extracellular vesicles, Biomaterials 271 (2021) 120742, https://doi.org/10.1016/j.biomaterials.2021.120742.
[26] K. Kida, T. Kanaki, S. Gao, D. Hatanaka, M. Iwakami, S. Liu, M. Horikawa, M. Ono, D. Chang, A novel 3D culture system using a chitin-based polysaccharide material produces high-quality allogeneic human UCMSCs with dispersed sphere morphology, Cells 11 (6) (2022) 995, https://doi.org/10.3390/cells11060995.
[27] Z. Cesarz, K. Tamama, Spheroid culture of mesenchymal stem cells, Stem Cell. Int. (2016) 9176357, https://doi.org/10.1155/2016/9176357, 2016.
[28] R. Pochampally, Colony forming unit assays for MSCs, Methods Mol. Biol. 449 (2008) 83–91, https://doi.org/10.1007/978-1-60327-169-1_6.
[29] N.A. Wright, Stem cell identification–in vivo lineage analysis versus in vitro isolation and clonal expansion, J. Pathol. 227 (3) (2012) 255–266, https://doi.org/10.1002/path.4018.
[30] S. Babazadeh, S. Mahdi Nassiri, V. Siavashi, M. Sahlabadi, M. Hajinasrollah, M. Z. Ahmadmahmudi, Macrophage polarization by MSC-derived CXCL12 determines tumor growth, Cell. Mol. Biol. Lett. 26 (1) (2021) 30, https://doi.org/10.1186/s11658-021-00273-w.
[31] X.Z. Yan, J.J. van den Beucken, S.K. Both, P.S. Yang, J.A. Jansen, F. Yang, Biomaterial strategies for stem cell maintenance during in vitro expansion, Tissue engineering. Part B, Reviews 20 (4) (2014) 340–354, https://doi.org/10.1089/ten.TEB.2013.0349.
[32] N.C. Cheng, S. Wang, T.H. Young, The influence of spheroid formation of human adipose-derived stem cells on chitosan films on stemness and differentiation capabilities, Biomaterials 33 (6) (2012) 1748–1758, https://doi.org/10.1016/j.biomaterials.2011.11.049.
[33] A. Jauković, D. Abadjieva, D. Trivanović, E. Stoyanova, M. Kostadinova, S. Pashova, S. Kestendjieva, T. Kukolj, M. Jeseta, E. Kistanova, M. Mourdjeva, Specificity of 3D MSC spheroids microenvironment: impact on MSC behavior and properties, Stem cell reviews and reports 16 (5) (2020) 853–875, https://doi.org/10.1007/s12015-020-10006-9.
[34] L. Tan, X. Liu, H. Dou, Y. Hou, Characteristics and regulation of mesenchymal stem cell plasticity by the microenvironment - specific factors involved in the regulation of MSC plasticity, Genes Dis 9 (2) (2020) 296–309, https://doi.org/10.1016/j.gendis.2020.10.006.
[35] M. Kozma, B. Acharya, R. Bissessur, Chitin, chitosan, and nanochitin: extraction, synthesis, and applications, Polymers 14 (19) (2022) 3989, https://doi.org/10.3390/polym14193989.
[36] C. Gilbert, T.C. Tang, W. Ott, B.A. Dorr, W.M. Shaw, G.L. Sun, T.K. Lu, T. Ellis, Living materials with programmable functionalities grown from engineered microbial co-cultures, Nat. Mater. 20 (5) (2021) 691–700, https://doi.org/10.1038/s41563-020-00857-5.
[37] W. Chen, P. Cao, Y. Liu, A. Yu, D. Wang, L. Chen, R. Sundarraj, Z. Yuchi, Y. Gong, H. Merzendorfer, Q. Yang, Structural basis for directional chitin biosynthesis, Nature 10 (7931) (2022) 402–408, https://doi.org/10.1038/s41586-022-05244-5.
[38] X. Zhang, J. Yuan, F. Li, J. Xiang, Chitin synthesis and degradation in Crustaceans: a genomic view and application, Mar. Drugs 19 (3) (2021) 153, https://doi.org/10.3390/md19030153.
[39] D. Hladik, I. Höfig, U. Oestreicher, J. Beckers, M. Matjanovski, X. Bao, H. Scherthan, M.J. Atkinson, M. Rosemann, Long-term culture of mesenchymal

stem cells impairs ATM-dependent recognition of DNA breaks and increases genetic instability, Stem Cell Res. Ther. 10 (1) (2019) 218, https://doi.org/10.1186/s13287-019-1334-6.
[40] W.B. Swanson, M. Omi, Z. Zhang, H.K. Nam, Y. Jung, G. Wang, P.X. Ma, N. E. Hatch, Y. Mishina, Macropore design of tissue engineering scaffolds regulates mesenchymal stem cell differentiation fate, Biomaterials 272 (2021) 120769, https://doi.org/10.1016/j.biomaterials.2021.120769.
[41] F. Pei, L. Ma, J. Jing, J. Feng, Y. Yuan, T. Guo, X. Han, T.V. Ho, J. Lei, J. He, M. Zhang, J.F. Chen, Y. Chai, Sensory nerve niche regulates mesenchymal stem cell homeostasis via FGF/mTOR/autophagy axis, Nat. Commun. 14 (1) (2023) 344, https://doi.org/10.1038/s41467-023-35977-4.
[42] D.H. Kim, Y. Wang, H. Jung, R.L. Field, X. Zhang, T.C. Liu, C. Ma, J.S. Fraser, J. R. Brestoff, S.J. Van Dyken, A type 2 immune circuit in the stomach controls mammalian adaptation to dietary chitin, Science 381 (6662) (2023) 1092–1098, https://doi.org/10.1126/science.add5649.
[43] S. Wang, L. Yang, B. Cai, F. Liu, Y. Hou, H. Zheng, F. Cheng, H. Zhang, L. Wang, X. Wang, Q. Lv, L. Kong, K.B. Lee, Q. Zhang, Injectable hybrid inorganic nanoscaffold as rapid stem cell assembly template for cartilage repair, Natl. Sci. Rev. 9 (4) (2022), https://doi.org/10.1093/nsr/nwac037 nwac037.
[44] I. Kelnar, L. Kaprálková, P. Němeček, J. Dybal, R.M. Abdel-Rahman, M. Vyroubalová, M. Nevoralová, A.M. Abdel-Mohsen, The effects of the deacetylation of chitin nanowhiskers on the performance of PCL/PLA bio-nanocomposites, Polymers 15 (14) (2023) 3071, https://doi.org/10.3390/polym15143071.
[45] I.V. Tyshkunova, I.V. Gofman, D.G. Chukhchin, A.V. Malkov, A.I. Mishanin, A. S. Golovkin, E.N. Pavlova, D.N. Poshina, Y.A. Skorik, Biophysical characterization and cytocompatibility of cellulose cryogels reinforced with chitin nanowhiskers, Polymers 14 (13) (2022) 2694, https://doi.org/10.3390/polym14132694.
[46] Y. Zhou, H. Chen, H. Li, Y. Wu, 3D culture increases pluripotent gene expression in mesenchymal stem cells through relaxation of cytoskeleton tension, J. Cell Mol. Med. 21 (6) (2017) 1073–1084, https://doi.org/10.1111/jcmm.12946.
[47] J.M. Santos, S. P Camões, E. Filipe, M. Cipriano, R.N. Barcia, M. Filipe, M. Teixeira, S. Simões, M. Gaspar, D. Mosqueira, D.S. Nascimento, P. Pinto-do-Ó, P. Cruz, H. Cruz, M. Castro, J.P. Miranda, Three-dimensional spheroid cell culture of umbilical cord tissue-derived mesenchymal stromal cells leads to enhanced paracrine induction of wound healing, Stem Cell Res. Ther. 6 (1) (2015) 90, https://doi.org/10.1186/s13287-015-0082-5.
[48] J.J. McGuire, J.S. Frieling, C.H. Lo, T. Li, A. Muhammad, H.R. Lawrence, N. J. Lawrence, L.M. Cook, C.C. Lynchcorresponding, Mesenchymal stem cell-derived interleukin-28 drives the selection of apoptosis resistant bone metastatic prostate cancer, Nat. Commun. 12 (2021) 723, https://doi.org/10.1038/s41467-021-20962-6.
[49] E.A. Ross, L.A. Turner, H. Donnelly, A. Saeed, M.P. Tsimbouri, K.V. Burgess, G.B. V. Jayawarna, Y. Xiao, M.A.G. Oliva, J. Willis, J. Bansal, P. Reynolds, J.A. Wells, J. Mountford, M. Vassalli, N. Gadegaard, R.O.C. Oreffo, M.S. Sanchez, M. J Dalby, Nanotopography reveals metabolites that maintain the immunomodulatory phenotype of mesenchymal stromal cells, Nat. Commun. 14 (1) (2023) 753, https://doi.org/10.1038/s41467-023-36293-7.
[50] C. Ma, X. Qi, Y. Wei, Z. Li, H. Zhang, H. Li, F. Yu, Y. Pu, Y. Huang, Y. Rena, Amelioration of ligamentum flavum hypertrophy using umbilical cord mesenchymal stromal cell-derived extracellular vesicles, Bioact. Mater. 19 (2023) 139–154, https://doi.org/10.1016/j.bioactmat.2022.03.042.
[51] H. Husseina, A. Kishena, Proteomic profiling reveals engineered chitosan nanoparticles mediated cellular crosstalk and immunomodulation for therapeutic application in apical periodontitis, Bioact. Mater. 11 (2022) 77–89, https://doi.org/10.1016/j.bioactmat.2021.09.032.
[52] J.A. Guadix, J. López-Beas, B. Clares, J.L. Soriano-Ruiz, J.L. Zugaza, P. Gálvez-Martín, Principal criteria for evaluating the quality, safety and efficacy of hMSC-based products in clinical practice: current approaches and challenges, Pharmaceutics 11 (11) (2019) 552, https://doi.org/10.3390/pharmaceutics11110552.
[53] F. Donnaloja, M.T. Raimondi, L. Messa, B. Barzaghini, F. Carnevali, E. Colombo, D. Mazza, C. Martinelli, L. Boeri, F. Rey, C. Cereda, R. Osellame, G. Cerullo, S. Carelli, M. Soncini, E. Jacchetti, 3D photopolymerized microstructured scaffolds influence nuclear deformation, nucleo/cytoskeletal protein organization, and gene regulation in mesenchymal stem cells, APL Bioeng. 7 (3) (2023) 036112, https://doi.org/10.1063/5.0153215.
[54] R.V. Desai, X. Chen, B. Martin, S. Chaturvedi, D.W. Hwang, W. Li, C. Yu, S. Ding, M. Thomson, R.H. Singer, R.A. Coleman, M.M.K. Hansen, L.S. Weinberger, A DNA repair pathway can regulate transcriptional noise to promote cell fate transitions, Science 373 (6557) (2021), https://doi.org/10.1126/science.abc6506 eabc6506.